Thermodynamics of the $ZnSO_4$ – H_2SO_4 – H_2O system

Vielma T.; Salminen, J.; Lassi, U.

Abstract

Internally consistent set of thermodynamic parameters was derived for the binary $ZnSO_4$–H_2O -system using the CALPHAD method. Available data on water activity, EMF measurements, solubility and heat of solution and dilution measurements was reviewed. Additional parameters for the ternary $ZnSO_4$–H_2SO_4–H_2O system were derived based on the available solubility and boiling point data. Solubility of zinc sulfate was predicted successfully under conditions relevant in hydrometallurgical processing of zinc, and even up to 15 mol/kg sulfuric acid solutions. Temperature dependent Pitzer parameters for the binary and ternary systems are reported.

1. Introduction

Understanding behavior of the $ZnSO_4$-H_2SO_4-H_2O system under a wide range of temperatures is important for the key stages of hydrometallurgical recovery of zinc: leaching, purification and electrowinning. The existing amount of data, however, is still not yet sufficient to cover all the complexities of the electrolytic zinc process. More data is required also with added minor components and their interactions. It has been shown by Königsberger et al [1-3] that using a suitable activity coefficient model, such as the Pitzer model, makes it possible to model thermodynamics of concentrated multicomponent electrolyte solutions of industrial relevance with great accuracy. Attempts to model the aqueous zinc sulfate system have been few, however.

Liu and Papangelakis [4] used mixed solvent electrolyte (MSE) model [5] to study O_2 – $ZnSO_4$ – H_2SO_4 – H_2O system from 25 to 250 °C. They used available solubility data and mean activity coeffients at 25°C to derive their model, and the accuracy of their model in predicting mean activity coefficients of solute species seems to be lacking, at least at low molalities and at 25 °C. Königsberger and Eriksson [6] used Pitzer model to calculate solubilities of different hydrates of zinc sulfate. Full details of their model, however, were not published. Guerra and Bestetti [7] have compiled data on the physicochemical properties of the $ZnSO_4$-H_2SO_4-H_2O system, and among them they presented temperature dependent Pitzer parameters, based on the temperature derivatives measured by Silvester and Pitzer [8]. Iliuta et al [9] used extended UNIQUAC formalism to model the $ZnSO_4$–H_2O system, among several others. Azimi

et al [10] used the MSE model for modelling $CaSO_4$–$ZnSO_4$–H_2O systems, from 25 to 90 °C, with a focus on the solubility of $CaSO_4$. A comprehensive treatment, involving water activities, mean activity coefficients, calorimetric measurements, properties of the solid phases and solubility data has not been published so far.

Modelling in this work was carried out using the FactSage thermochemical modelling software [11]. With the OptiSage optimisation module, CALPHAD method was used to derive a thermodynamically sound and internally consistent model based on measurement data.

2. Literature Data

Phase boundaries

Solubilities of different zinc sulfate hydrates have been studied systemically and reported as early as the late 19th century by Callendar and Barnes [12] and Cohen [13]. Callendar and Barnes [12] studied solubility of zinc sulfate from 0 to 50 °C using electromotive force measurements. The change in hydration state from heptahydrate to hexahydrate was later stressed by Barnes [14]. Bury [15] studied solubilities of the hexahydrate from 11 to 61.1 °C and metastable monoclinic heptahydrate from 7 to 23 °C. Bury [15] also noted a likely error that Cohen [13] made in identifying the solid phases, mistaking the metastable monoclinic heptahydrate for the hexahydrate.

The reported solubilities for heptahydrate and hexahydrate agree remarkably well. Solubility of zinc sulfate monohydrate, however, has been studied to a lesser extent and serious discrepancies between reported solubilities exists. Values reported by Schröder [16], Rudolph et al [17] and Benrath [18] agree moderately at lower temperatures, but near 100 °C their results deviate from each other. Solubilities given by Söhnel and Novotny [19] seem to fall on an entirely different curve. The reason for these differences and likely errors is possibly kinetic effects as stated by Bury [15]. It should be noted, however, that for the reported solubilities at high temperatures, for which equilibration should be considerably faster, the same discrepancies exist.

Solubility and thermodynamics of zinc sulfate in aqueous solutions of sulfuric acid has been studied in startlingly few publications, considering how important this system is for hydrometallurgical recovery of zinc as well as recovery of by-product metals from any zinc bearing solutions. Copeland and Short [17] studied solubility of zinc sulfate in 0 to 97 wt-% sulfuric acid solutions, from -4.5 to 70 °C. Balarew et al [18] studied the solubility in 10 to 97 wt-% sulfuric acid solutions, from 15 to 80 °C.

Brown and Prue [22] measured freezing point depressions of very dilute aqueous zinc sulfate solutions. CRC Handbook [23] lists freezing point depressions up to 1.18 mol kg^{-1} solutions. Bruni [24] reported -

6.4 °C as the eutectic temperature. Agde and Schimmel [25] observed the eutectic point at 2.30 mol kg^{-1} and -6.55 °C.

Li et al [26] reported boiling points of $ZnSO_4$ and $ZnSO_4$–H_2SO_4 solutions up to 3.5 molal $ZnSO_4$ and 4 molal H_2SO_4, under pressures ranging from 0.3 to 1.01 bar.

Barieau and Giauque [27] reported peritectic temperature between heptahydrate and hexahydrate at 311.28 K in agreement with values from Cohen et al [13], 311.29 and 311.27 K. Barieau and Giauque [27] reported peritectic temperature between hexahydrate and monohydrate at 333.45 K, while Benrath [18] reported a clearly lower temperature, 328.65 K. Balarew et al [21] reported a considerably higher temperature 343.15 K, highlighting the before mentioned discrepancy concerning the monohydrate. Grønvold and Meisingset [28] reported 311.3 and 327.65 K as the peritectic temperatures.

Activity measurements

Activity measurements of zinc sulfate solutions have been carried out on a wide range of concentrations but only at a few temperatures. Robinson and Jones [29] measured vapor pressures of zinc sulfate solution from 0.1 to 3.6 molal at 298.15 K, reporting the osmotic coefficients. Apelblat [30] measured vapor pressures of saturated zinc sulfate solutions between 288.67 and 311.40 K. Albright et al [31] carried out isopiestic measurements at 298.15 K at concentrations from 0.1004 to 4.3092 molal. Bray [32] measured mean activity coefficients of $ZnSO_4$ for 0.00001 to 3.5 molal solutions at 298.15 K using electromotive force measurements.

Miladinović et al [33] carried out isopiestic measurements at 298.15 K for solutions from 1.3506 to 3.0217 molal, reporting the osmotic coefficients. Guendouzi et al [34] used the hygrometric method to measure water activity at 298.15 K from 0.2 to 3.0 molal solutions. Yang et al [35,36] measured osmotic coefficients of zinc sulfate solutions at 323.15 and 373.15 K using the isopiestic method.

Calorimetric measurements

Enthalpies of formation for aqueous $ZnSO_4$ have been listed in the NBS Tables [37] from infinite dilution to 3.7 molal solutions. Giauque et al [38] reported relative partial molar enthalpies of zinc sulfate solutions from 1 to 3.6 molal at 298.15 K and heat capacities from 0.7 to 3.6 molal at 298.15 and 308.15 K. Lange et al [39] measured heats of dilution of zinc sulfate solutions from 1 M to 0.00005 M.

Barieau and Giaque [27] measured heat capacities of the solid heptahydrate and hexahydrate from 15 to 310 K. Kelley [40] reported heat capacity of the monohydrate at 282.15 K. Pan and Tremaine [41] reported heat capacity of aqueous zinc ion Zn^{2+}(aq) at infinite dilution from 283.15 to 328.15 K.

3. Optimisation & Modelling

Water vapour was modelled as a real gas, using the Tsonopoulos correlation [42] and data in the FactSage Pure Substances database [11]. All solid phases were modelled as pure substances. For modelling aqueous solutions, Pitzer model [43] incorporating the Harvie-Weare modification [44] was used. Pitzer model is one most used activity coefficient models for aqueous solutions, and typically applicable up to 6 mol/kg H_2O electrolyte solutions. Harvie and Weare [44] showed that by including unsymmetrical electrostatic mixing in the model, the models fit in multicomponent systems can be improved.

In the Pitzer model, the osmotic coefficient of the solvent water in a solution of a general, mixed electrolyte is expressed as [45]:

$$\phi - 1 = \left(\frac{2}{\sum_i m_i}\right)\left\{\begin{array}{l} If^{\phi} + \sum_c \sum_a m_c m_a \left[B_{ca}^{\phi} + ZC_{ca}\right] \\ + \sum_{c<} \sum_{c'} m_c m_{c'} \left[\Phi_{cc'}^{\phi} + \sum_a m_a \psi_{cc'a}\right] \\ + \sum_{a<} \sum_{a'} m_a m_{a'} \left[\Phi_{aa'}^{\phi} + \sum_c m_c \psi_{aa'c}\right] \end{array}\right\} \quad (1)$$

where

$$f^{\phi} = -A_{\phi}\left[\frac{I^{1/2}}{1 + bI^{1/2}}\right] \quad (2)$$

$$B_{\mathrm{MX}}^{\phi} = \beta_{\mathrm{MX}}^{(0)} + \beta_{\mathrm{MX}}^{(1)}\exp(-\alpha_1 I^{1/2}) + \beta_{\mathrm{MX}}^{(2)}\exp(-\alpha_2 I^{1/2}) \quad (3)$$

$$Z = \sum_i m_i |z_i| \quad (4)$$

$$C_{\mathrm{MX}} = \frac{C_{\mathrm{MX}}^{\phi}}{2|z_{\mathrm{M}} z_{\mathrm{X}}|^{1/2}} \quad (5)$$

$$\Phi_{ij}^{\phi} = \Phi_{ij} + I\Phi'_{ij} \quad (6)$$

and m_i is the molality of species i, with indexes c and a referring to cations and anions, I is the ionic strength in molality basis, A_ϕ is the Debye-Hückel coefficient for the osmotic coefficient. $\beta_{\mathrm{MX}}^{(i)}$ and C_{MX}^{ϕ} are the binary Pitzer interaction parameters typically reported in literature. b = 1.2, α_1 = 1.4 and α_2 = 12

for 2-2 electrolytes, for other types $\alpha_1 = 2.0$. α_2 is not needed since $\beta_{MX}^{(2)}$ is included only for 2-2 electrolytes. Φ_{ij} and ψ_{ijk} are the so-called mixing terms, arising from interactions between like-charged ions. The apostrophe here indicates differentiation with respect to I. Φ_{ij} can be further expressed as a sum of two parts θ_{ij} and ${}^{E}\theta_{ij}(I)$, where the first term is taken as a constant (at constant temperature and pressure) and accounts for short range interactions between species i and j. The latter part corresponds to unsymmetrical electrostatic mixing effects and depends on the charges of i and j, the total ionic strength and solvent properties (hence, also temperature and pressure).

For the mean activity coefficient of electrolyte $M_{\nu M}X_{\nu X}$, the corresponding equations are:

$$\begin{aligned}\ln \gamma_{\pm} \quad = \quad & |z_M z_X| F + \frac{\nu_M}{\nu}\sum_a m_a \left[2B_{Ma} + ZC_{Ma} + \frac{2\nu_X}{\nu_M}\Phi_{Xa}\right] \\ & + \frac{\nu_X}{\nu}\sum_c m_c \left[2B_{cX} + ZC_{cX} + \frac{2\nu_M}{\nu_X}\Phi_{Mc}\right] \\ & + \sum_c\sum_a m_c m_a \left[\frac{2\nu_M z_M}{\nu} C_{ca} + \frac{\nu_M}{\nu}\psi_{Mca} + \frac{\nu_X}{\nu}\psi_{caX}\right] \\ & + \sum_{c<}\sum_{c'} m_c m_{c'} \frac{\nu_X}{\nu}\psi_{cc'X} + \sum_{a<}\sum_{a'} m_a m_{a'} \frac{\nu_M}{\nu}\psi_{Maa}\end{aligned} \tag{7}$$

where

$$F = f^{\gamma} + \sum_c\sum_a m_c m_a B'_{ca} + \sum_{c<}\sum_{c'} m_c m_{c'}\Phi_{cc'} + \sum_{a<}\sum_{a'} m_a m_{a'}\Phi_{aa'} \tag{8}$$

$$f^{\gamma} \quad = \quad -A_{\phi}\left[\frac{I^{1/2}}{1 + bI^{1/2}} + \frac{2}{b}\ln\left(1 + bI^{1/2}\right)\right] \tag{9}$$

$$B_{MX} \quad = \quad \beta_{MX}^{(0)} + \beta_{MX}^{(1)} g(\alpha_1 I^{1/2}) + \beta_{MX}^{(2)} g(\alpha_2 I^{1/2}) \tag{10}$$

$$B'_{MX} \quad = \quad \beta_{MX}^{(0)} + \beta_{MX}^{(1)} g'(\alpha_1 I^{1/2}) + \beta_{MX}^{(2)} g'(\alpha_2 I^{1/2}) \tag{11}$$

$$g(x) \quad = \quad \frac{2(1 - (1 + x)e^{-x})}{x^2} \tag{12}$$

$$g'(x) \quad = \quad -\frac{2\left(1 - (1 + x + \frac{x^2}{2})e^{-x}\right)}{x^2} \tag{13}$$

For the binary $ZnSO_4$-H_2O system, equations (1) and (7) can be simplified to following form [46]:

$$\phi - 1 \quad = \quad 4f^{\phi} + mB^{\phi}_{\mathrm{MX}} + m^2 C^{\phi}_{\mathrm{MX}} \tag{14}$$

$$\ln\gamma_{\pm} \quad = \quad 4f^{\gamma} + m(B^{\phi}_{\mathrm{MX}} + B_{\mathrm{MX}}) + \frac{3}{2}m^2(C^{\phi}_{\mathrm{MX}}) \tag{15}$$

Taking appropriate derivatives, Pitzer model can be used to calculate enthalpies and heat capacities of solution [8]. In this work, data for 2-2 electrolytes only was used. Relative apparent molar enthalpy ${}^{\phi}L$ and apparent molar heat capacity ${}^{\phi}C_P$ for 2-2 electrolytes are defined as follows

$${}^{\phi}L \quad = \quad \frac{4A_L}{b}\ln(1 + bI^{1/2}) - 2RT^2(mB^{L}_{\mathrm{MX}} + 2m^2 C^{L}_{\mathrm{MX}}) \tag{16}$$

$$B^{L}_{\mathrm{MX}} \quad = \quad \beta^{(0)L}_{\mathrm{MX}} + \beta^{(1)L}_{\mathrm{MX}} g(\alpha_1 I^{1/2}) + \beta^{(2)L}_{\mathrm{MX}} g(\alpha_2 I^{1/2}) \tag{17}$$

$$\beta^{(\mathrm{i})L}_{\mathrm{MX}} \quad = \left(\frac{\partial \beta^{(\mathrm{i})}_{\mathrm{MX}}}{\partial T}\right)_P \tag{18}$$

$$C^{L}_{\mathrm{MX}} \quad = \frac{1}{4}\left(\frac{\partial C^{\phi}_{\mathrm{MX}}}{\partial T}\right)_P \tag{19}$$

$${}^{\phi}C_P \quad = \quad C^{\mathrm{o}}_{P,\mathrm{MX}} + \frac{4A_J}{b}\ln(1 + bI^{1/2}) - 2RT^2\left(mB^{J}_{\mathrm{MX}} + 2m^2 C^{J}_{\mathrm{MX}}\right) \tag{20}$$

$$B^{J}_{\mathrm{MX}} \quad = \quad \beta^{(0)L}_{\mathrm{MX}} + \beta^{(1)J}_{\mathrm{MX}} g(\alpha_1 I^{1/2}) + \beta^{(2)J}_{\mathrm{MX}} g(\alpha_2 I^{1/2}) \tag{21}$$

$$\beta^{(\mathrm{i})J}_{\mathrm{MX}} \quad = \left(\frac{\partial^2 \beta^{(\mathrm{i})}_{\mathrm{MX}}}{\partial T^2}\right)_P + \frac{2}{T}\left(\frac{\partial \beta^{(\mathrm{i})}_{\mathrm{MX}}}{\partial T}\right)_P \tag{22}$$

$$C^{J}_{\mathrm{MX}} = \frac{1}{4}\left(\frac{\partial^2 C^{\phi}_{\mathrm{MX}}}{\partial T^2}\right)_P + \frac{1}{2}\left(\frac{\partial C^{\phi}_{\mathrm{MX}}}{\partial T}\right)_P \quad (23)$$

A_L and A_J are the Debye-Hückel coefficients for enthalpy and heat capacity, respectively.

$$A_L = 4RT^2\left(\frac{\partial A_\phi}{\partial T}\right)_P \quad (24)$$

$$A_J = \left(\frac{\partial A_L}{\partial T}\right)_P \quad (25)$$

In order to calculate thermodynamic properties of the system in a wide temperature range, temperature dependent expressions for the Pitzer parameters and heat capacities of all constituents have to be assumed. In FactSage, temperature dependency of the Pitzer interaction parameters *P* is modelled using expression:

$$P(T) = \frac{p_1}{T} + p_2 + p_3 \ln T + p_4 T + p_5 T^2 + \frac{p_6}{T^2} \quad (26)$$

Heat capacities of each species were modelled using the following type of equation:

$$C_P(T) = c_1 + c_2 T + c_3 T^2 + \frac{c_4}{T^2} \quad (27)$$

Optimisation of the model parameters was carried out using FactSage optimiser, OptiSage, which is designed for fitting thermodynamic parameters to measurement data using a Bayes algorithm [11]. Table 1 shows the data chosen for the final optimisation. Data for the optimisation was chosen from the reviewed literature based on the apparent quality and accuracy of measurements. Due to the large scatter of experimental solubility data above 380 K, they were exluded from the optimisation. Reported uncertainties of the measured data were used for the fitting when available. Otherwise the uncertainties were estimated from the consistency of the data and the experimental method utilised. Lack of freezing point depression data of solutions beyond 1.2 mol kg^{-1} lead us to investigate it ourselves up to reported solubilities of the heptahydrate.

Table 1. Data selected for the optimisation of the $ZnSO_4$-H_2O system. All data in the given references

was used in the optimization.

Data type	*T* range /K	*m* range / mol kg^{-1}	Number of points	Ref.
Activity of water	298.15-373.15	0 – 4.3	168	[29,31,33,35,36]
Freezing point depression	266.85 – 273.15	0 – 2.42	27	[23], This work
Boiling point elevation	373.15 – 375.28	0 – 3.5	10	[26]
Solubility of $ZnSO_4 \cdot 7\ H_2O$	268.15 – 310.15	2.44 – 4.21	16	[13,14,16]
Solubility of $ZnSO_4 \cdot 7\ H_2O$(monoclinic)	280.78 – 296.09	3.29 – 3.84	7	[15]
Solubility of $ZnSO_4 \cdot 6\ H_2O$	284.50 – 329.25	3.66 – 5.04	18	[14-16]
Solubility of $ZnSO_4 \cdot\ H_2O$	333.15 – 373.15	3.64 – 4.67	15	[16-18]
Enthalpy of dilution	298.15	0 – 3.7	28	[37]
Heat capacity of solution	298.15 – 308.15	0.77 – 3.55	12	[38]

4. Experimental

Zinc sulfate heptahydrate (≥99.0 %, Sigma-Aldrich) was purified two times by re-crystallisation from water. Experiments were performed both with the re-crystallised heptahydrate and monohydrate, made by drying the heptahydrate at 105°C for 24 h. Dehydration to monohydrate was verified by weighing. Solutions ranging from 0.6 to 2.4 mol kg^{-1} were prepared by weighing. Double distilled water was used throughout the experiments.

Freezing point depression experiments were performed using a custom-made apparatus. It consisted of a hollow glass vessel, connected to cooling liquid circulation (water–ethanol mixture), a magnetic stirrer, and an insulating lid, through which an electronic thermometer was placed into the solution. Cooling was controlled by changing the circulation rate of the cooling liquid.

During the measurements, the temperature of the solution was recorded every few seconds. As ice started to crystallise, a sudden rise in temperature was noted, after which the temperature started to decrease slowly again. Nucleation was achieved either spontaneously or by increased agitation or addition of small ice crystals. Freezing point was taken as the highest temperature reached. Several measurements were performed for each solution at varying degrees of undercooling. The “true” freezing point was estimated by linear extrapolation to zero undercooling. Table 2 shows the estimated freezing points and the respective uncertainties estimated from the extrapolation.

Table 2. Estimated freezing points and their estimated uncertainties.

m / mol kg^{-1}	T / K
0.988	271.23 ± 0.13
1.263	270.68 ± 0.11
1.608	269.99 ± 0.23
1.994	268.68 ± 0.26
2.038	268.49 ± 0.22
2.248	267.08 ± 0.41
2.420	267.07 ± 0.08
2.429	267.30 ± 0.33
2.438	266.85 ± 0.48
2.503	266.92 ± 0.37

5. Results and discussion

The heat capacity of aqueous zinc ion Zn^{2+}(aq) was calculated using the revised HKF model [47,48] in its simplified pressure-independent form. The two solute-specific parameters, c_1 and c_2, of the simplified revised HKF model were fitted to available literature data [41]. The resulting heat capacity function was then split to two temperature intervals and refitted to more convenient polynomial form, equation (27), which FactSage can utilize. Figure 1 shows comparison between calculated heat capacities and literature values. Heat capacity function from the SUPCRT92 database [49] is also shown for comparison. Heat capacity functions for H_2O and SO_4^{2-}- and HSO_4^- -ions were taken from literature [50,51]. The selected thermodynamic functions for the sulfate species correspond to the Okuwaki K_2-equation [52].

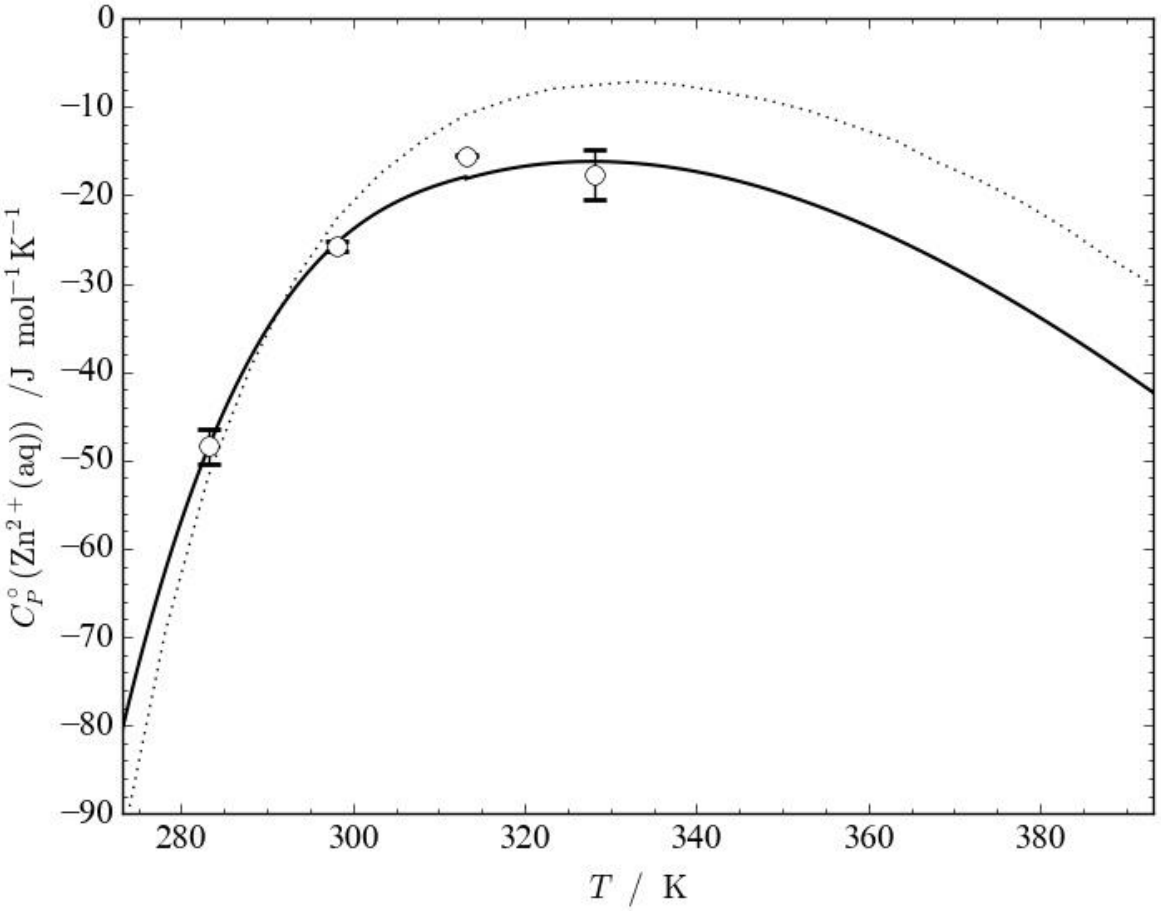

Fig. 1. The heat capacity of Zn^{2+}(aq) ion as a function of temperature. Solid line: this work; dotted line: SUPCRT92[45]; ○ Pan & Tremaine [41]

Heat capacity functions of the solid zinc sulfate phases were fitted to existing data in the literature. Data for hexahydrate and heptahydrate was taken from Barieau & Giaque [27]. The heat capacity of the monohydrate, however, is insufficiently studied. The only found reported value is that of Kelley [40], 34.7 cal mol^{-1} K^{-1} at 282 K. Heat capacity was extrapolated to higher temperatures as suggested by DeKock [53]. Table 3 shows coefficients of the heat capacity function for all species considered in this work, along with their respective temperature ranges.

Table 3. Coefficients for the heat capacity function. C_P functions of the condensed phases are applicable down to at least 266.72 K, the calculated eutectic temperature. Functions for SO_4^{2-} and

HSO_4^- ions are valid down to 283.15 K [57], for Zn^{2+} the lower limit is 273.15 K.

	T_{max}	c_1	c_2	$c_3 \cdot 10^3$	$c_4 \cdot 10^{-7}$
H^+ [a]	-	0	0	0	0
$H_2O(l)$[b]	298.15	134.4	-0.3859	0.6294	0
	373.15	-89.81	-0.0943	0.153	0
	500	311.953	-0.8588	0.8951	-0.55991
$Zn^{2+}(aq)$	313.15	23410.788	-98.23394	116.0188	-39.65541
	443.15	1331.4489	-3.654225	2.090997	-4.023608
$SO_4^{2-}(aq)$[c]	328.15	46200.6	-186.8004	211.929	-85.4629
	403.15	1080.77	-0.7188	-3.9917	-6.7658
	448.15	5857.78	-10.7722	0	-29.0789
$HSO_4^-(aq)$[c]	328.15	48246.05	-197.6415	227.731	-85.4629
	403.15	3126.22	-11.5599	11.8103	-6.7658
	448.15	7903.23	-21.6133	158.02	-29.0789
$H_2O(s)$[b]	273.15	2.1127	0.1305	0	0
$ZnSO_4 \cdot 7\ H_2O$ (s)	400	68.92271	1.048365	0	0
$ZnSO_4 \cdot 6\ H_2O$ (s)	400	53.02976	1.014761	0	0
$ZnSO_4 \cdot H_2O$ (s)	400	38.99488	0.376560	0	0

[a] By convention

[b] Kobylin [50]

[c] Sippola [51]

Thermodynamic properties of the aqueous species, water and ice were taken from literature [51,54,55] and excluded from optimisation. Table 4 shows their standard enthalpies of formation and standard entropies at 298.15 K. Properties of the solid zinc sulfate phases at 298.15 K, however, were refined in this work, using the Pitzer model described below. Exception was $S°$ of the heptahydrate, for which the calorimetric value determined by Barieau and Giauque [27] was accepted. For the hexahydrate, it was

necessary to adjust the value slightly from the calorimetric result [27]. Table 5 shows the refined values in comparison with literature values. Good comparison was found between this work and literature data.

Table 4. Standard enthalpies of formation and standard entropies at 298.15 K for the aqueous species, water and ice.

	$\Delta_f H°$ / kJ mol^{-1}	$S°$ / J mol^{-1} K^{-1}	Ref.
H^+ (aq)	0	0	By convention
H_2O(l)	-285.83	69.95	[54]
Zn^{2+} (aq)	-153.39	-109.80	[54]
SO_4^{2-} (aq)	-909.34	18.5	[54]
HSO_4^- (aq)	-885.2	137.5	[51]
H_2O(s)	-292.74	44.78	[55]

Table 5. Standard enthalpies of formation and standard entropies of the solid zinc sulfate phases at 298.15 K. Values from this work compared to literature.

$\Delta_f H°$ / kJ mol^{-1}			$S°$ / J mol^{-1} K^{-1}			
$ZnSO_4·7H_2O$	$ZnSO_4·6H_2O$	$ZnSO_4·H_2O$	$ZnSO_4·7H_2O$	$ZnSO_4·6H_2O$	$ZnSO_4·H_2O$	Ref.
-3076.62	-2776.40	-1303.69	388.69[a]	363.36	137.74	This work
-3077.75	-2777.46	-1304.49	388.7	363.6	138.5	[37]
-	-	-	388.69	363.59	-	[27]
-3077.54	-2777.76	-1304.78	-	-	-	[53]

[a] Value was taken from [23] and excluded from optimisation

Temperature dependent Pitzer parameters for the Zn^{2+}–SO_4^{2-} binary were optimised using the water activities, freezing point depressions, boiling point elevations, enthalpy of dilution and heat capacity of solution data, shown in Table 1. A good fit to all used experimental data was achieved by considering only the p_1 and p_2 parameters for $\beta^{(0)}$, $\beta^{(2)}$ and C^{ϕ}. For $\beta^{(1)}$, it was necessary to include also parameters p_4 and p_5. Table 6 shows the optimised temperature dependent Pitzer parameters. Calculated value of each parameter at 25 °C is also included. Values reported by Pitzer and Mayorga [46] are shown for

comparison.

Table 6. Optimised Pitzer parameters for the Zn^{2+}– SO_4^{2-} binary. Calculated values at 25 °C are compared to values reported by Pitzer and Mayorga [46].

P	p_1	p_2	p_4	p_5	P(25 °C)	Pitzer & Mayorga
$\beta^{(0)}_{ZnSO4}$	-112.68525	0.5468214	0	0	0.1689	0.1949
$\beta^{(1)}_{ZnSO4}$	-17455.620	156.87770	-0.45039814	0.0004408657	3.325	2.883
$\beta^{(2)}_{ZnSO4}$	21332.288	-109.50287	0	0	-37.95	-32.81
C^{ϕ}_{ZnSO4}	59.798086	-0.16347515	0	0	0.0370	0.0290

Pitzer and Mayorga [46] reported 0.005 – 3.5 molal as the range of validity for their parametrisation, extending essentially to saturated solutions at 25 °C. Figure 2 shows comparison between activity of water predicted by their model, the present model and experimental data [29,31,33,35,36]. As can be seen, the two models are almost identical when the zinc sulfate molality is below 3. In more concentrated solutions, the present model seems to be more accurate. This is because data from Albright et al [31], extending up to 4.3 molal supersaturated solutions, was included in our optimisation process.

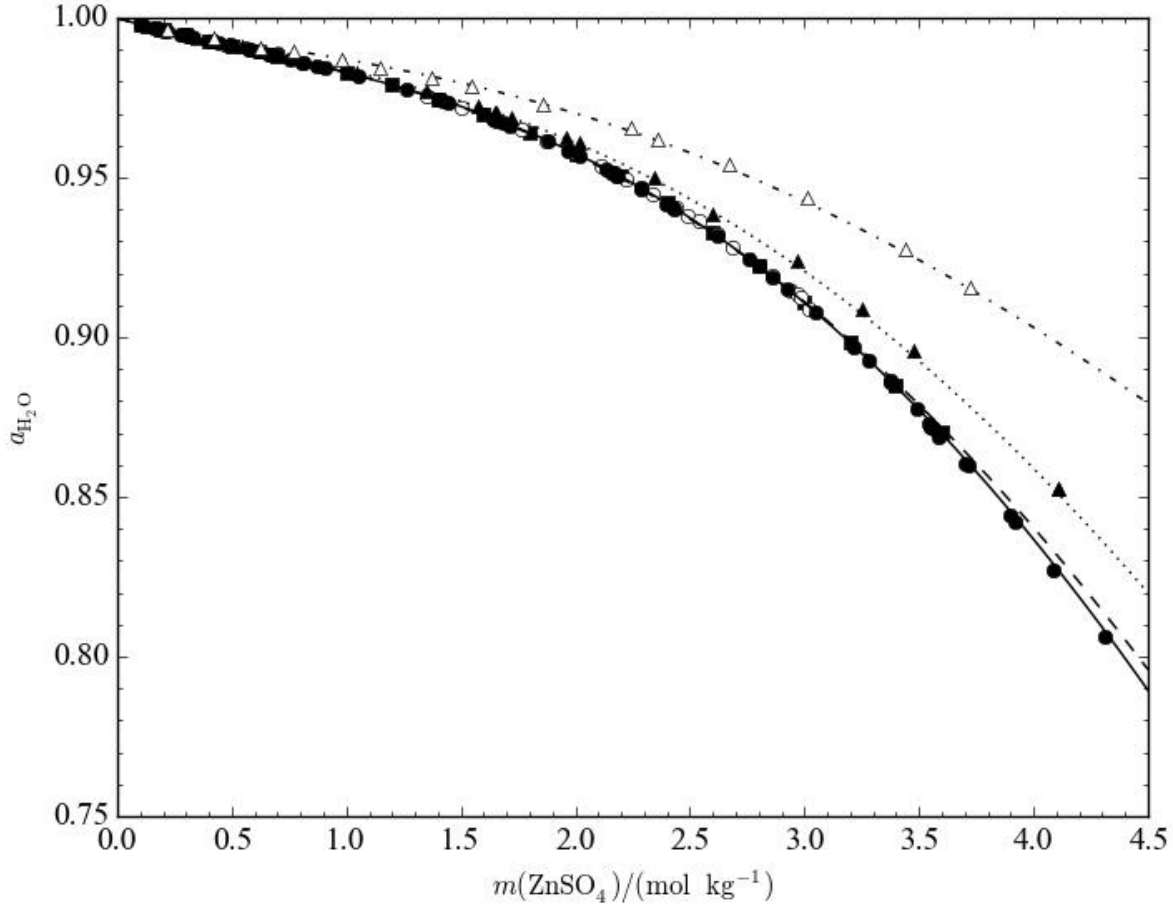

Fig. 2. Activity of water at 298.15 K as a function of $ZnSO_4$ molality. Calculated: Solid line, this work at 298.15 K; dashed line, Pitzer and Mayorga [46] at 298.15 K; dotted line, this work at 323.15 K; dash-dot line, this work at 373.15 K. Experimental: ■ Robinson and Jones [29], ○ Miladinovic et al [33], ● Albright et al [31], ▲ Yang et al [35] at 323.15 K, Δ Yang et al [36] 373.15 K.

Enthalpy and heat capacity

Derivatives of the Pitzer parameters with respect to temperature can be used to calculate the relative apparent molar enthalpy of the solution. Table 7 shows the derivatives calculated in this work at 298.15 K and those reported by Königsberger and Eriksson [6] and Silvester and Pitzer [8]. Figure 3 shows the calculated relative apparent molar enthalpies as functions of molality, with the three listed sets of parameters. Experimental points [37-39] are shown for comparison.

Calculated results from Königsberger and Eriksson [6] are comparable to ours. It is clear, however, that the parameters given by Silvester and Pitzer [8] are not valid above 1 mol kg^{-1}, as also pointed out by Königsberger and Eriksson [6].

Table 7. Comparison of temperature derivatives of the Pitzer parameters.

P	This work	Silvester & Pitzer [8]	Königsberger & Eriksson [6]
$\beta^{(0)L}_{ZnSO4}$	$1.27\cdot10^{-3}$	$-3.66\cdot10^{-3}$	$6.7\cdot10^{-4}$
$\beta^{(1)L}_{ZnSO4}$	$8.86\cdot10^{-3}$	$2.33\cdot10^{-2}$	$1.297\cdot10^{-2}$
$\beta^{(2)L}_{ZnSO4}$	$-2.4\cdot10^{-1}$	$-3.33\cdot10^{-1}$	$-3.15\cdot10^{-1}$
C^{L}_{ZnSO4}	$-6.73\cdot10^{-4}$	$9.9\cdot10^{-4}$	$-1.16\cdot10^{-4}$

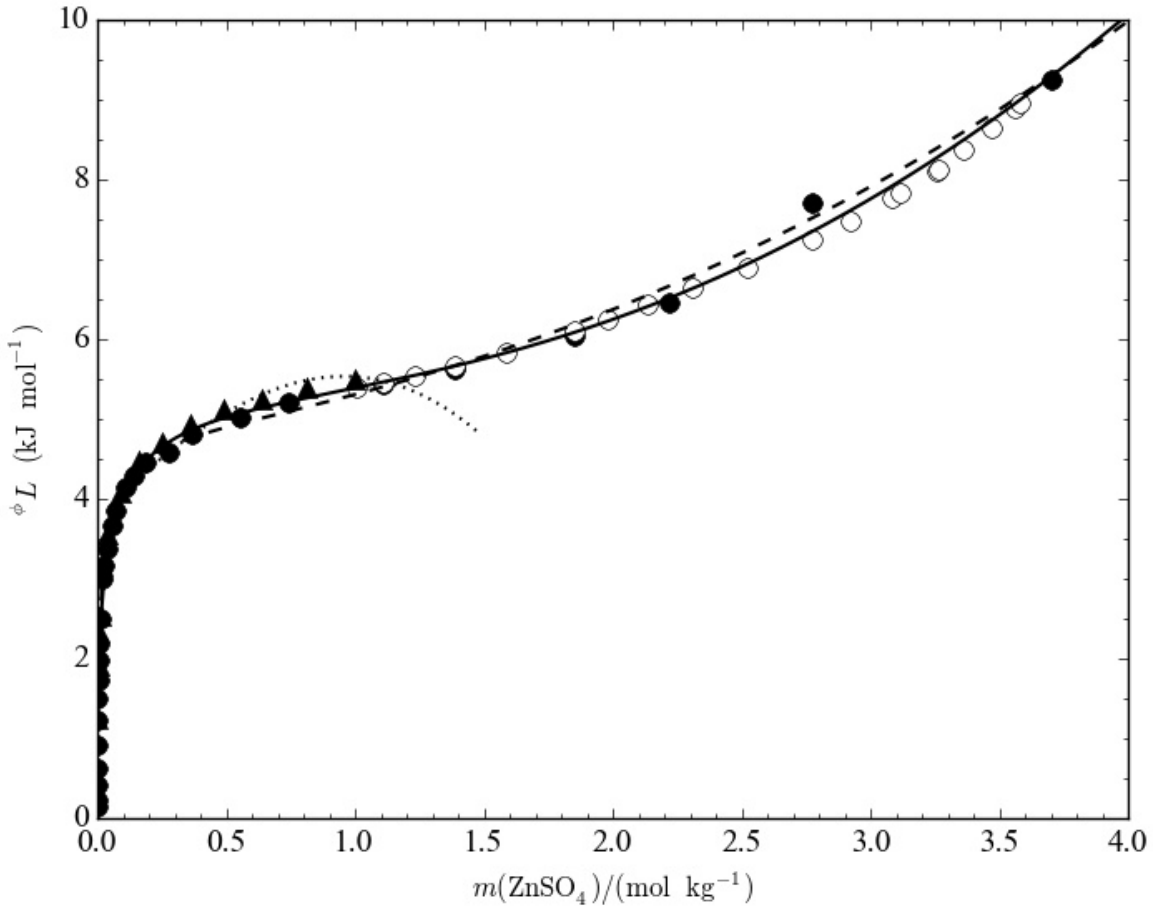

Fig. 3. Apparent relative molar enthalpy as a function of $ZnSO_4$ molality. Calculated: – This work, -- Königsberger and Eriksson [6], ⋯ Silvester and Pitzer [8]. Experimental: ● NBS tables [37], ○ Giauque et al [38], ▲ Lange et al [39]. Data from [38] and [39] were not used in the optimisation.

Figure 4 shows calculated heat capacity of solution compared to experimental data by Giauque et al [38] at 298.15 K. Equally good fit was achieved at 308.15 K. For a more complete model, however, heat capacities of the solution should be measured on a wider composition range with multiple measurements below 0.1 mol kg^{-1}. Measurements at high temperatures should also be done to extend and test the model.

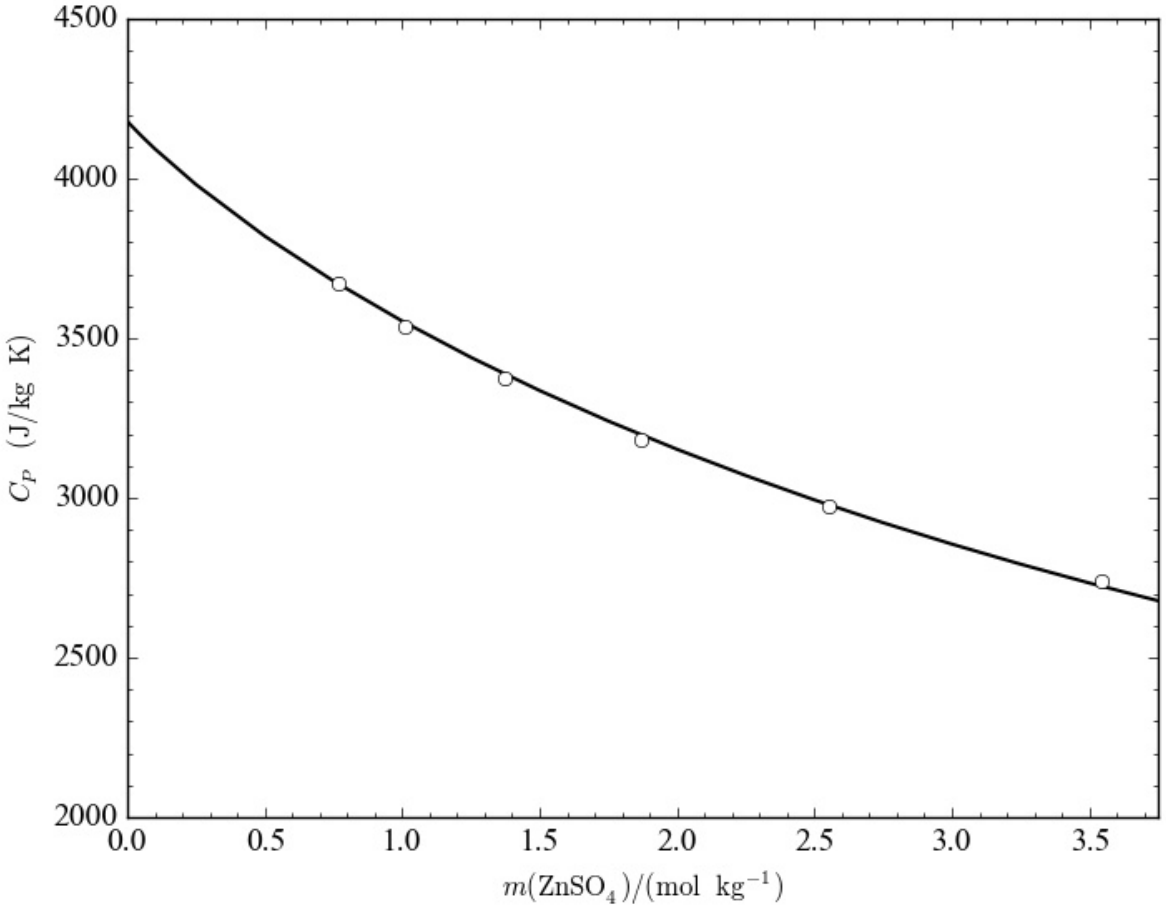

Fig. 4. Heat capacity of solution at 298.15 K. Experimental: ○ Giauque et al [38].

Phase diagram

Figure 5 shows the calculated phase diagram for the binary $ZnSO_4$ – H_2O system from 260 to 400 K at 1.01325 bar, along with experimental data of the phase boundaries. The overall fit to measured data is good. The present model predicts the peritectic point between heptahydrate and hexahydrate at 4.29 mol kg^{-1}, 311.03 K. This compares well with literature, 311.28 K on average [12,27,28]. The peritectic point between hexahydrate and monohydrate is predicted to lie at 4.79 mol kg^{-1}, 324.67 K. Agreement with literature is only moderate due to wide range of estimates of the peritectic temperature, from 327 to 343

K.

Figure 6 shows a magnification around the eutectic point. The eutectic point in this work was predicted at 2.36 mol kg^{-1}, 266.72 K. This compares well with the eutectic temperature 266.76 K reported by Bruni [24] and the eutectic point 2.30 mol kg^{-1}, 266.6 K reported by Agde and Schimmel [25]. A good overall fit was achieved with the data measured in this work, despite the rather large experimental uncertainties associated with the method. However, with the OptiSage optimiser, it was possible to account for these uncertainties. It should also be pointed out that the calculated freezing curve of water in this work coincides almost exactly with those calculated for $NiSO_4$, $FeSO_4$ and $MnSO_4$ [50,57,58].

The monohydrate clearly shows larger scatter in regards of experimental data than the heptahydrate or the hexahydrate. However, as will be shown below, current model successfully predicts solubility of the monohydrate in concentrated sulfuric acid solutions, from 268.65 to 353.15 K. Extrapolation to high temperatures is uncertain due to the large scatter of existing experimental data. Extrapolation also results in solubilities a lot smaller than reported experimental ones, with differences as large as 2 mol kg^{-1} above 400 K. It is still curious that the predicted curve has a distinct S-shape, where the solubility first decreases sharply with increasing temperature and then almost plateaus above 420 K, feature common to nickel(II), iron(II) and manganese(II) sulfate monohydrates [50,57,58]. Whether or not zinc sulfate actually follows similar trend, should be verified by new more careful experiments with longer equilibration times.

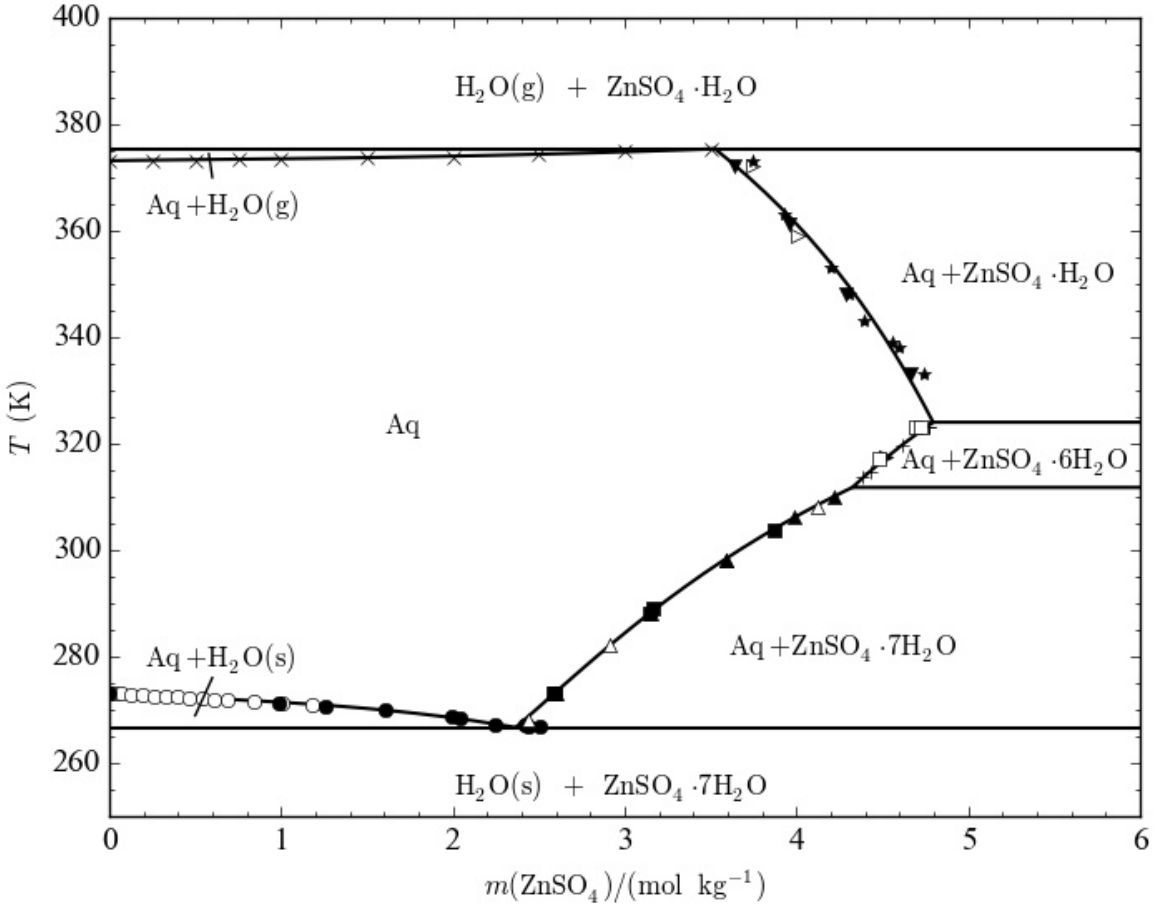

Fig. 5. Phase diagram of the $ZnSO_4$ – H_2O system at 1.01325 bar, and the phase data used in optimisation. Freezing point curve: ● This work, ○ CRC Handbook [23]. Heptahydrate solubility: ■ Barnes [14], ^ Cohen [13], ▲ Schröder [16]. Hexahydrate solubility: ► Bury [15], + Barnes [14], □ Schröder [16]. Monohydrate solubility: > Schröder [16], ▼ Rudolph [17], * Benrath [18]. Boiling point curve: × Li et al [26].

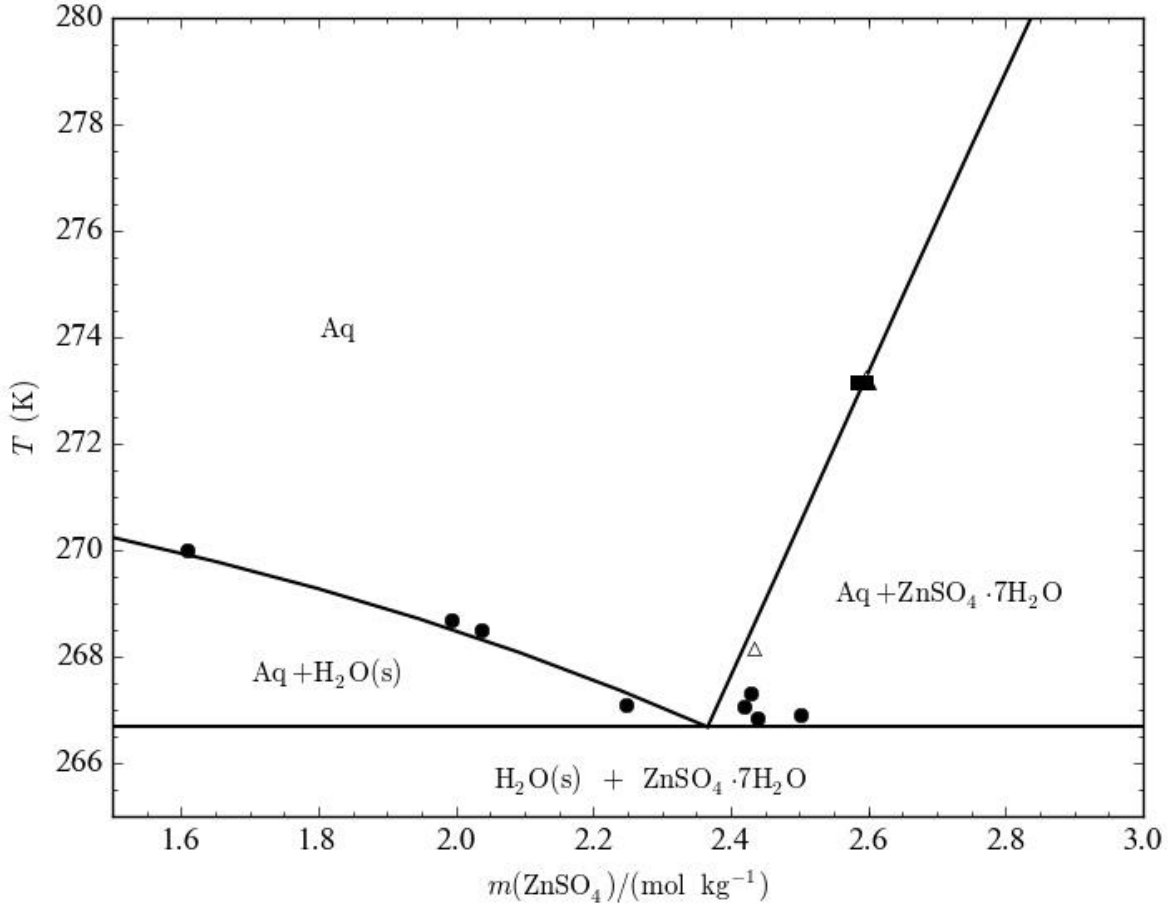

Fig. 6. Close-up of the eutectic point. Freezing point curve: ● This work. Heptahydrate solubility: ■ Barnes [14], ^ Cohen [13], ▲ Schröder [16].

The metastable monoclinic heptahydrate

Solubility data of monoclinic heptahydrate from Bury [15] was used to estimate its standard enthalpy of formation and standard entropy at 298.15 K. Its heat capacity was assumed to behave identically to the more common orthorhombic heptahydrate. This lead to $\Delta_f H°$ = (-3072.26±0.26) kJ mol^{-1} and $S°$ = (401.24±0.89) kJ mol^{-1} K^{-1}. Unfortunately, no direct measurements of these quantities have been reported to be compared to. Figure 7 shows the calculated metastable solubility curves of the monoclinic heptahydrate and hexahydrate and the respective experimental solubilities.

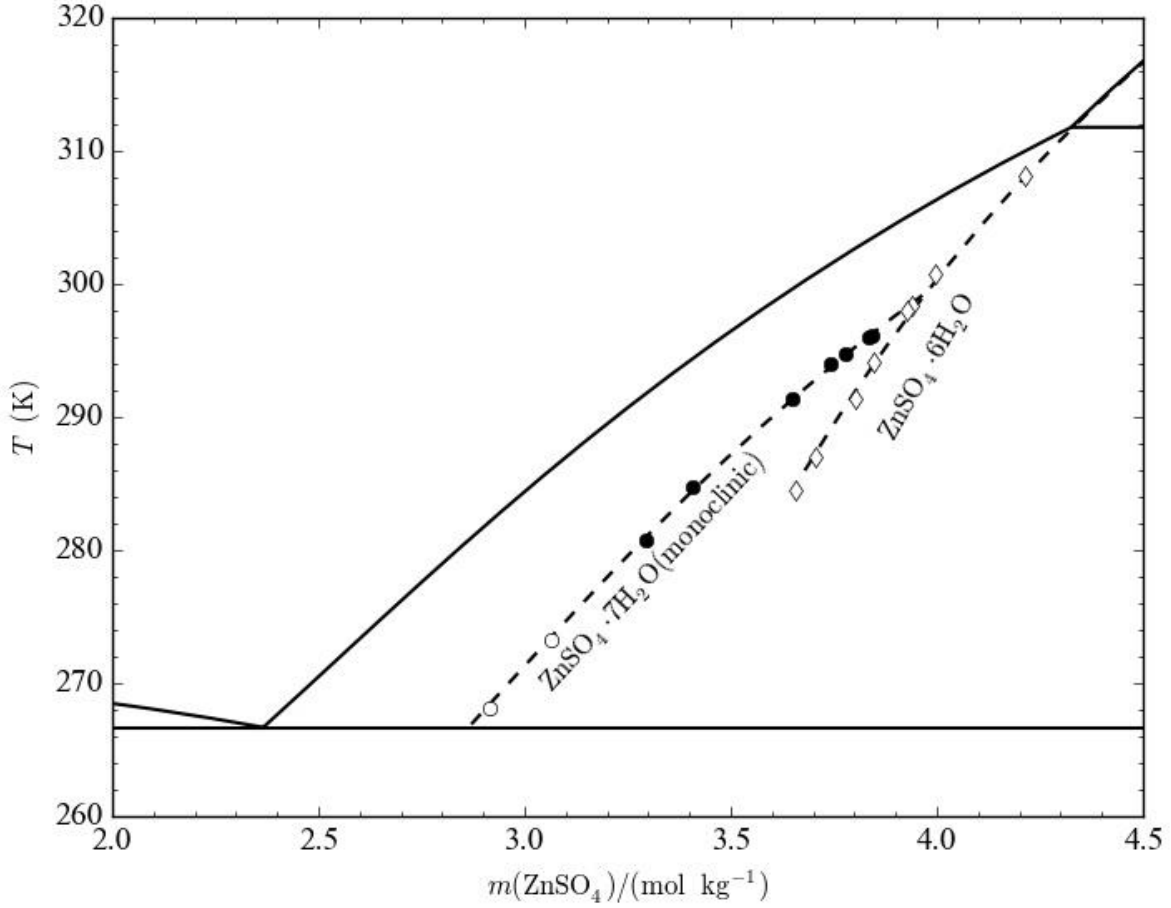

Fig. 7. Calculated: **- - -** Metastable solubility curves of monoclinic zinc sulfate heptahydrate and hexahydrate. Experimental: ● Bury [15], ◊ Bury [15], ○ Cohen [13]. Data from [13] was not used in the optimisation.

The ternary system $ZnSO_4$–H_2SO_4–H_2O

For industrial applications, $ZnSO_4$–H_2SO_4–H_2O is a more important system than the pure binary system discussed up till now. Process solutions in zinc recovery can contain up to 150 g H_2SO_4 dm^{-3}, which leads to a substantial concentration of hydrogen sulfate ions. Thus Zn^{2+}–HSO_4^- binary forms an important subsystem that has to be considered for a proper description of the whole system. Pitzer parameters for the Zn^{2+}–HSO_4^- binary were optimised using available solubility data of heptahydrate and hexahydrate [20] and boiling point data [26] of the ternary $ZnSO_4$–H_2SO_4–H_2O system. Pitzer parameters for the H_2SO_4-H_2O -system were taken from Sippola [59], the chosen parametrisation corresponds to Okuwaki K_2-equation [52] and parameter set A in Sippola's paper.

Good agreement with measurements was achieved with fitting just the p_1 and p_2 parameters for the Pitzer

parameters of the Zn^{2+}– HSO_4^- binary. Table 8 shows optimised parameters defined in this work, and the chosen parameter set for the H_2SO_4-H_2O -system.

Table 8. Pitzer parameters for the Zn^{2+}– HSO_4^- binary optimised in this work, and Pitzer parameters for the system H_2SO_4-H_2O [59].

P	p_1	p_2	P(25 °C)
$\beta^{(0)}_{Zn\text{-}HSO4}$	204.4621	-0.294233	0.3915
$\beta^{(1)}_{Zn\text{-}HSO4}$	1894.431	-1.29925	5.055
$C^{\phi}_{Zn\text{-}HSO4}$	-30.2551	0.099531	-0.00195
$\beta^{(0)}_{H\text{-}SO4}$	20.48760	-0.04083	0.0279
$C^{\phi}_{H\text{-}SO4}$	-42.79400	0.18522	0.0417
$\beta^{(0)}_{H\text{-}HSO4}$	54.14100	0.02808	0.2097
$\beta^{(1)}_{H\text{-}HSO4}$	147.75900	-0.00516	0.4904

Figures 8, 9, 10 and 11 show isothermal sections of the $ZnSO_4$–H_2SO_4–H_2O phase diagram at 268.65, 308.15, 343.15 and 353.15 K, respectively. Figure 12 shows the calculated boiling point curves in comparison to experimental data [26]. Our present model predicts solubility of zinc sulfate in aqueous sulfuric acid solutions reliably up to 15 mol H_2SO_4/kg H_2O and from -4.5 to 80°C. Testing of the model at higher temperatures is limited solely by the available solubility data. However, the predicted boiling point curves deviate slightly, 0.4-0.6 K below the experimental values at higher sulfuric acid and zinc sulfate concentrations. This could be solved by adding new temperature coefficients in binary Zn^{2+}-HSO_4^- parameters. New measurements for the solubilities at elevated temperatures are under way, however, to determine whether a more complicated temperature dependency of the Zn^{2+}-HSO_4^- parameters is actually necessary.

It should be noted that solubilities of only heptahydrate and hexahydrate, as reported by Copeland et al [20], were used in the optimisation, underlining the extrapolation capability of our model. After all, these data were limited to ~7.5 molal sulfuric acid solutions. For future work, it is suggested that solubilities up to at least 373 K are measured. For a more complete thermodynamic description, heat capacities and volumetric properties of the solution should also be measured in wide temperature and molality ranges.

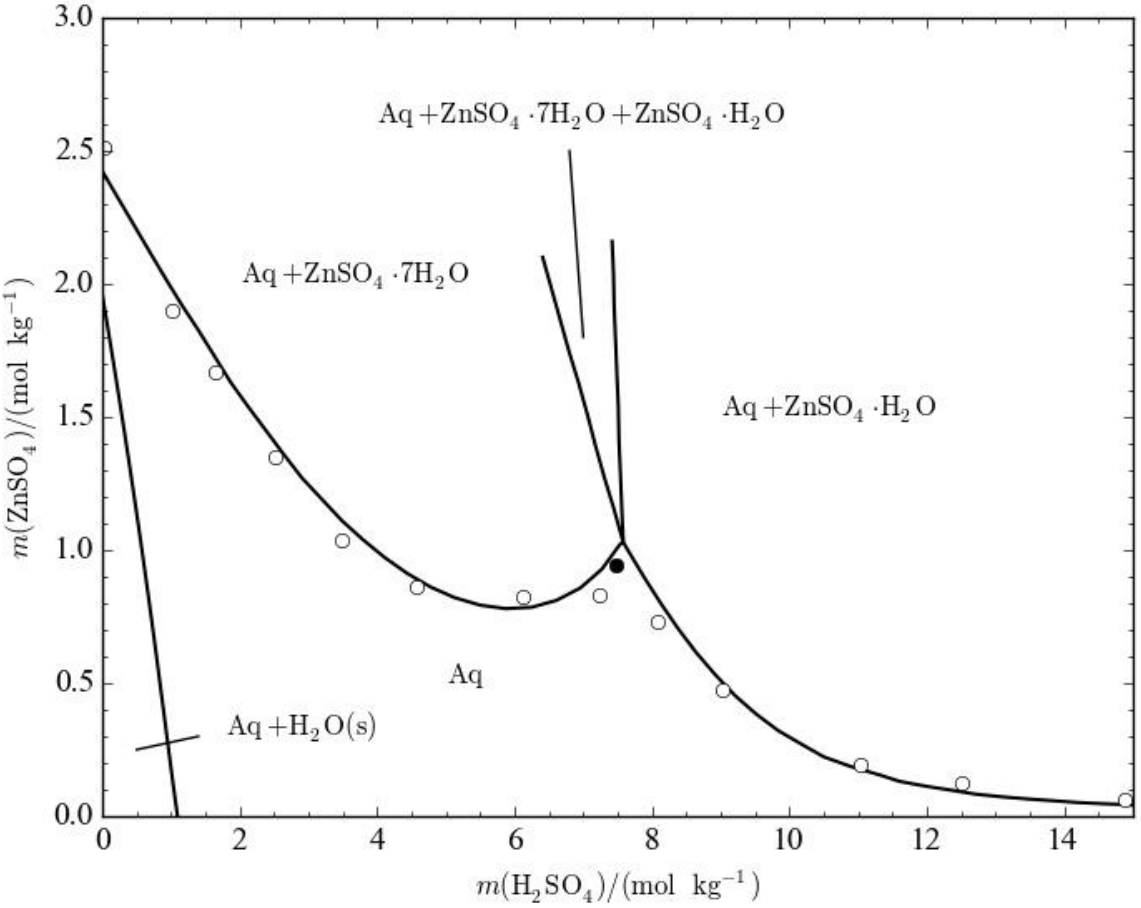

Fig. 8. Isothermal phase diagram of the $ZnSO_4$ – H_2SO_4 – H_2O system at 268.65 K. Phase boundaries between the two- and three-phase fields are only partially shown. Experimental: ○ solubility of single solid phase [20], ● peritectic point [20].

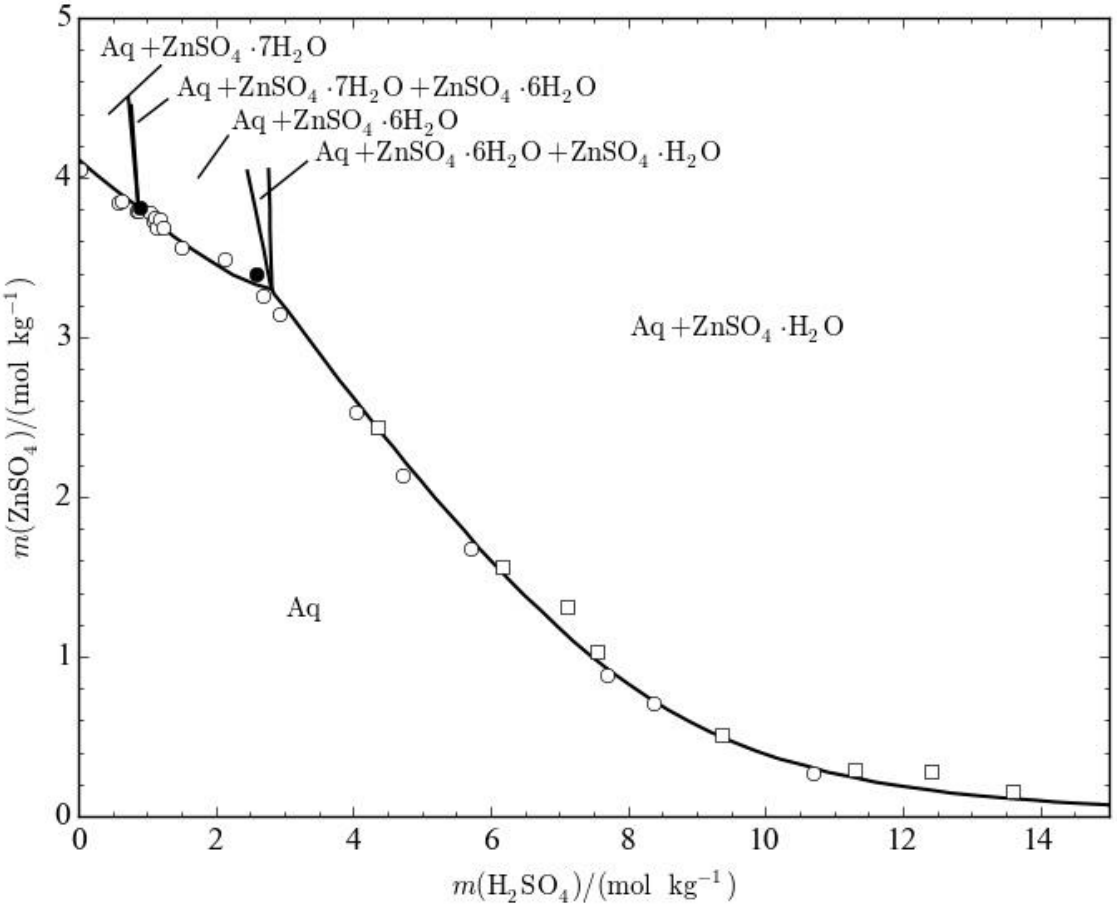

Fig. 9. Isothermal phase diagram of the $ZnSO_4$ – H_2SO_4 – H_2O system at 308.15 K. Phase boundaries between the two- and three-phase fields are only partially shown. Experimental: ○ solubility of single solid phase [20], ● peritectic points [20], □ Balarew et al [21]. Data from [21] was not used in the optimisation.

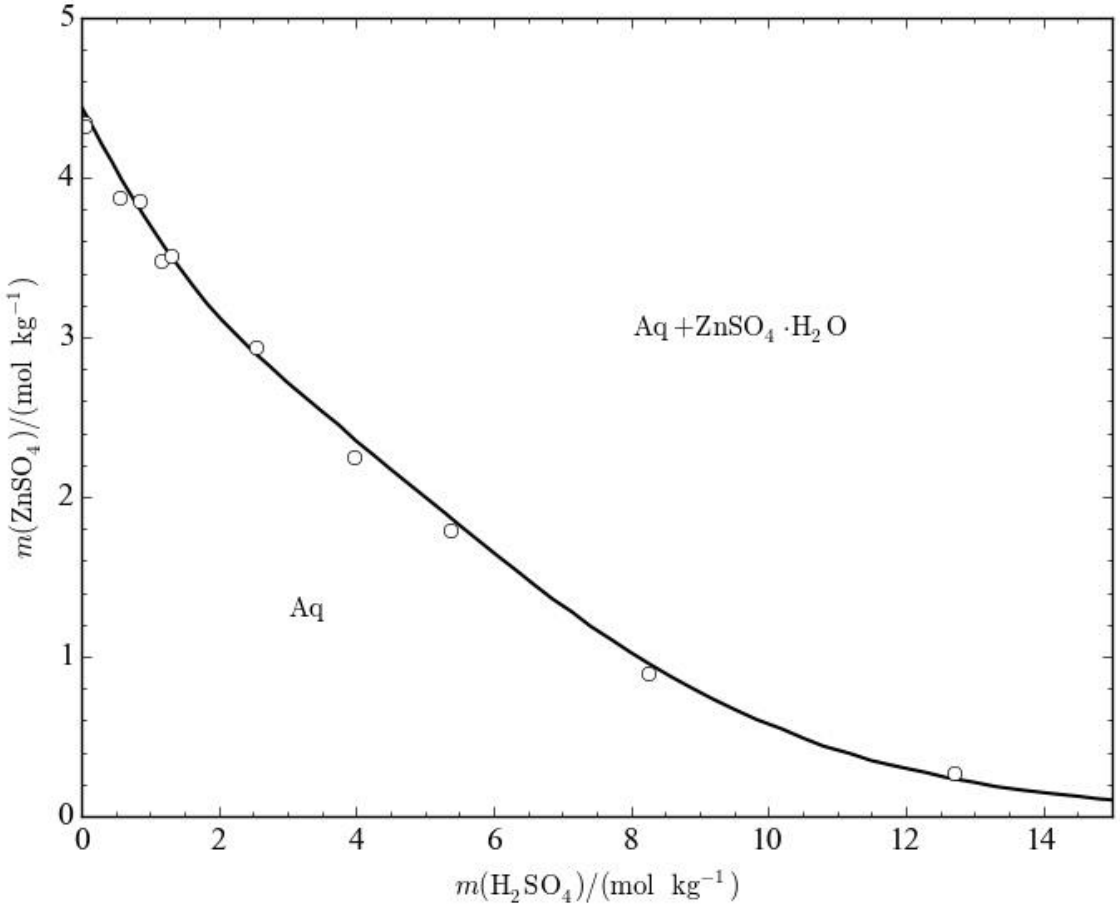

Fig. 10. Isothermal phase diagram of the $ZnSO_4$ – H_2SO_4 – H_2O system at 343.15 K. Experimental: ○ solubility of $ZnSO_4 \cdot H_2O$ [20]. None of the points shown were used in the optimisation.

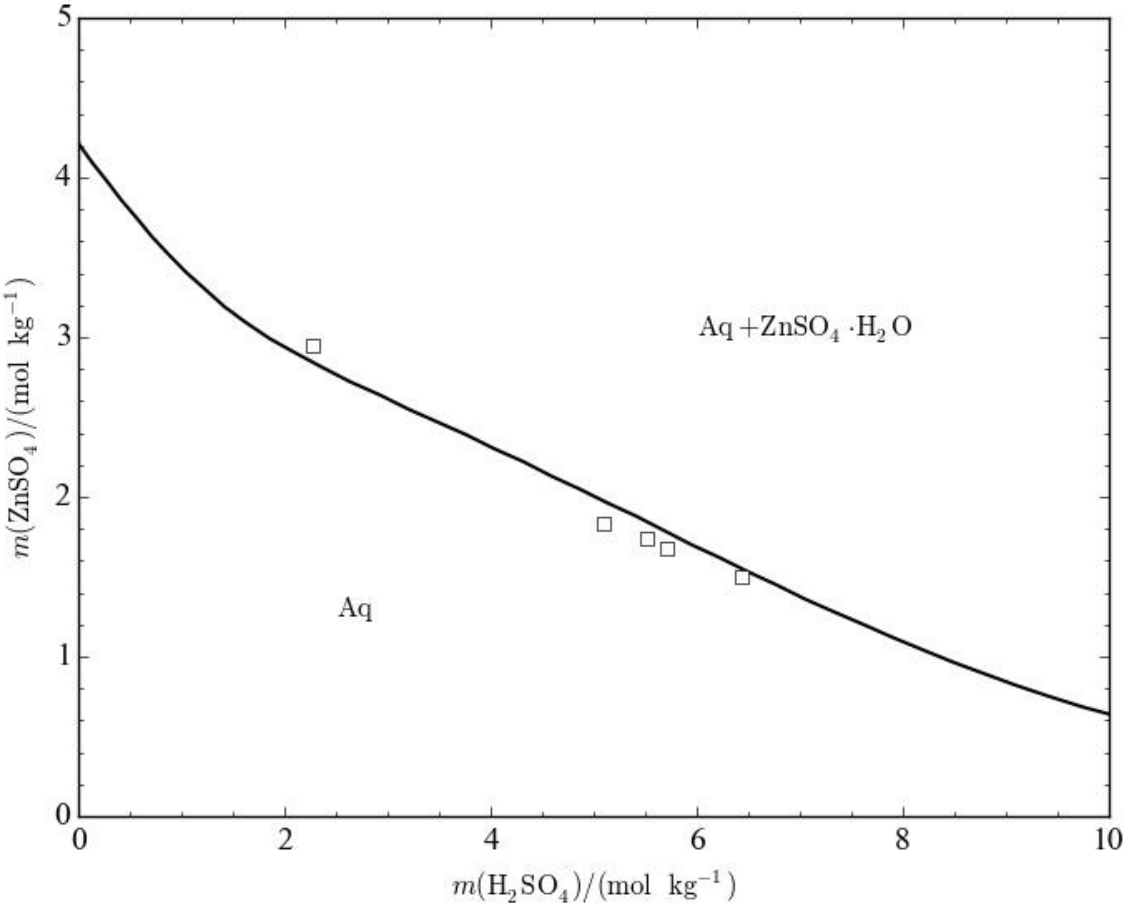

Fig. 11. Isothermal phase diagram of the $ZnSO_4$ – H_2SO_4 – H_2O system at 353.15 K. Experimental: □ solubility of $ZnSO_4 \cdot H_2O$ [21]. None of the points shown were used in the optimisation.

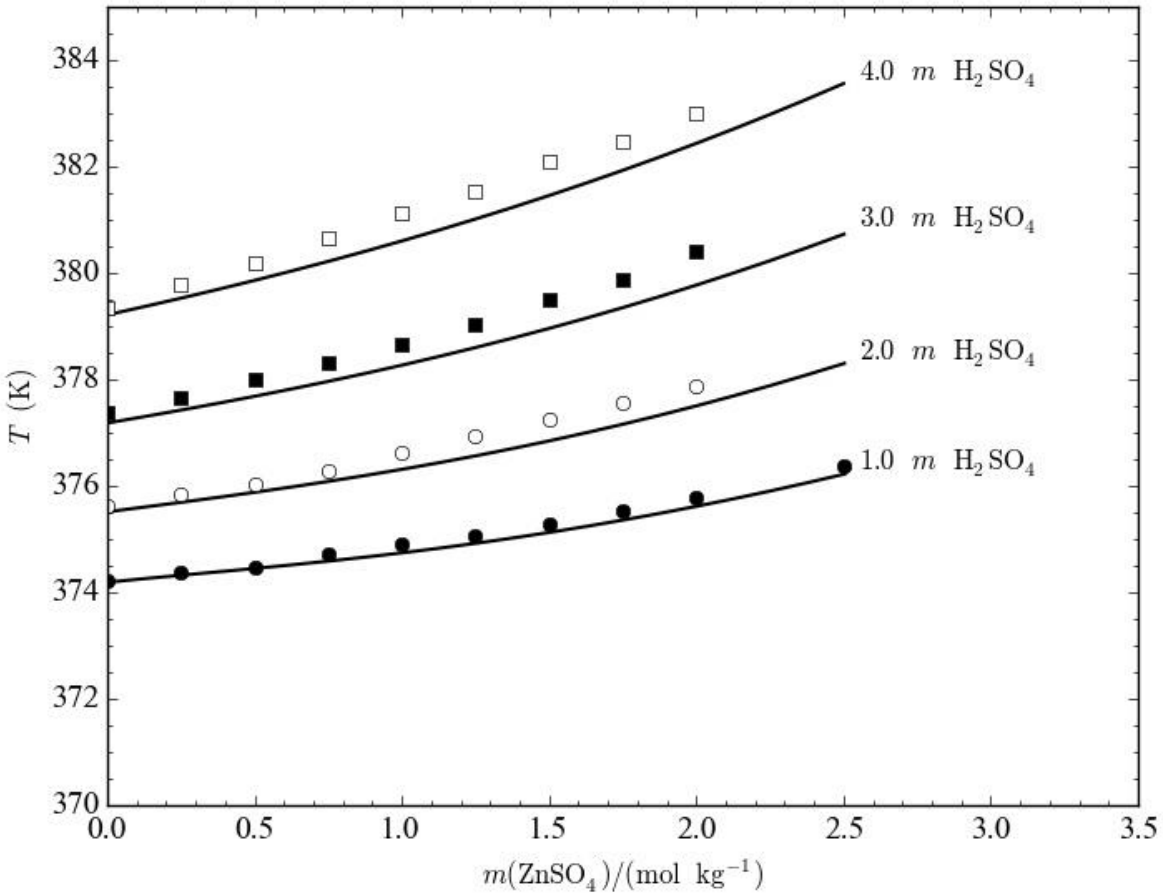

Fig. 12. Boiling points for aqueous $ZnSO_4$-H_2SO_4 solutions at different solute molalities. Symbols are experimental data points from Li et al [26].

6. Conclusions

An internally consistent thermodynamic model was presented for the binary $ZnSO_4$–H_2O and ternary $ZnSO_4$–H_2SO_4–H_2O systems. Good agreement with experimental data was achieved from 266 to 375 K and up to 15 mol H_2SO_4 kg^{-1}. Towards the end of this work, Höffler et al [60] published a temperature dependent modified Pitzer model for the $ZnSO_4$-H_2O system, including also temperature dependent expressions for the solubility products of the solid phases. Their modified Pitzer model included additional parameters $\beta^{(3)}_{ZnSO4}$ and α_3 as well as adjusted values for α_1 and α_2 to improve the accuracy of calculated osmotic coeffiecients at both low and high molalities. The difference in accuracy with the present model is clear, but not significant, at least concerning calculation of water activities and phase

equilibria. The present model also includes only 10 temperature coefficients for the Pitzer equations, whereas the model proposed by Höffler et al has 15. It should also be mentioned that Höffler et al used 3-5 more temperature coefficients for fitting solubility products of each solid phase. In this work the same was achieved by fitting and refining the values of standard enthalpies of formation and standard entropies of the solid phases, at 298.15 K.

To further improve the present model, heat capacity of the monohydrate should be measured at least up to 400 K. Also, heat capacity of the aqueous zinc ion at infinite dilution should be determined at higher temperatures. In addition, solubility of the monohydrate should be re-determined. For a complete thermodynamic treatise of the ternary system, heat capacities and volumetric properties of the solution should be determined on a wide range of conditions. Further work will be carried out by extending the model to describe important aspects of zinc process solutions.

7. Supporting info

Isothermal sections of the $ZnSO_4$-H_2SO_4-H_2O phase diagram at several temperatures are given in the supplementary data file.

8. Acknowledgements

Tekes/Adchem project is acknowledged for financial support. We thank two anonymous reviewers for their constructive comments, which lead to great improvements in the quality of this manuscript.

Literature Cited

1. Königsberger E, Eriksson G, May PM, Hefter G (2005) Ind Eng Chem Res **44**: 5805-5814.
2. Königsberger E, Bevis S, Hefter G, May PM (2005) J Chem Eng Data **50:** 1270-1276.
3. Königsberger E, May PM, Hefter G (2006) Monatsh Chem **137:** 1139-1149.
4. Liu H, Papangelakis VG (2005) Fluid Phase Equilibria **234:** 122-130.
5. Wang P, Anderko A, Young RD (2002) Fluid Phase Equilibria **203:** 141-176.
6. Königsberger E, Eriksson G (1995) Calphad **19:** 207-214.
7. Guerra E, Bestetti M (2006) **51:** 1491-1497.
8. Silvester LF, Pitzer KS (1977) J Phys Chem **81:** 1822-1828.
9. Iliuta MC, Thomsen K, Rasmussen P (2002) AlChE **48:** 2664-2689.
10. Azimi G, Papangelakis VG, Dutrizac JE 2007 Fluid Phase Equilibria **260:** 300-315.
11. Bale CW, Bélisle E, Chartrand P, Decterov SA, Eriksson G, Hack K, Jung IH, Kang YB, Melançon J, Pelton DA, Robelin C, Petersen S (2009) Calphad **33:** 295-311.
12. Callendar HL, Barnes HT (1897) Proc Roy Soc **62:** 117-152.
13. Cohen E (1900) Zeitschrift für Physikalische Chemie **34:** 179-186.
14. Barnes HT (1900) J Phys Chem **4:** 1-20.
15. Bury CR (1924) J Chem Soc Trans **125:** 2538-2541.
16. Schröder W (1936) Zeitschrift für anorganishce und allgemeine Chemie **228:** 129-159.

17. Rudolph WW, Brooker MH, Tremaine PR (1999) J Solution Chem **28:** 621-630.
18. Benrath A (1931) Zeitschrift für anorganishce und allgemeine Chemie **195:** 247-254.
19. Söhnel O, Novotny P (1985) *Densities of Aqueous Solutions of Inorganic Substances*, Elsevier, Amsterdam.
20. Copeland LC, Short OA (1940) J Am Chem Soc **62:** 3285-3291.
21. Balarew C, Trendafelov D, Gerganova M (1971) Monatsh Chem **102:** 465-473.
22. Brown PGM, Prue JE (1955) Proc R Soc Lond A **232:** 320-336.
23. Haynes WM (ed) (2012) *CRC Handbook of Chemistry and Physics*, 93rd Edition, page 5-148. CRC Press, Boca Raton.
24. Bruni G (1897) Gazz Chim Ital **1:** 537.
25. Agde G, Schimmel F (1928) Angewandte Chemie **41:** 340-341.
26. Li G, Zhang Y, Asselin E, Li Z (2014) J Chem Eng Data **59:** 3349-3460.
27. Barieau RE, Giauque WF (1950) J Am Chem Soc **72:** 5676-5684.
28. Grønvold F, Meisingset KK (1982) J Chem Thermodyn **14:** 1083-1098.
29. Robinson RA, Jones RS (1936) J Am Chem Soc **58:** 959-961.
30. Apelblat A (1992) J Chem Thermodynamics **24:** 619-626.
31. Albright JG, Rard JA, Serna S, Summers EE, Yang MC (2000) J Chem Thermodynamics **32:** 1447-1487.
32. Bray UB (1927) J Am Chem Soc **49:** 2372-2380.
33. Miladinović J, Todorović M, Ninković R (2002) J Chem Thermodynamics **34:** 1769-1776.
34. Guendouzi MEL, Mounir A, Dinane A (2003) J Chem Thermodynamics **35:** 209-220.
35. Yang H, Zeng D, Voigt W, Hefter G, Liu S, Chen Q (2014) J Chem Eng Data **59:** 97-102.
36. Yang H, Zeng D, Voigt W, Chen Y, Zhou Q (2016) J Chem Eng Data **61:** 3406-3412.
37. Wagman DD, et al (1982) J Phys Chem Ref Data **11:** Supplement No 2.
38. Giauque WF, Barieau RE, Kunzler JE (1950) J Am Chem Soc **72:** 5685-5690.
39. Lange E, Monheim J, Robinson AL (1933) J Am Chem Soc **52:** 4733-4744.
40. Kelley KK (1960) Bureau of Mines Bulletin.
41. Pan P, Tremaine PR (1994) Geochim Cosmochim Acta **58:** 4867-4874.
42. Tsonopoulos C (1974) AlChE J **20:** 263-272.
43. Pitzer KS (1973) J Phys Chem **77:** 268-277.
44. Harvie CE, Weare, JH (1980) Geochim Cosmochim Acta **44:** 981-997.
45. Pitzer KS, Kim JJ (1974) J Am Chem Soc **96:** 5701-5707.
46. Pitzer KS, Mayorga G (1974) J Solution Chem **3:** 539-546.
47. Helgeson HC, Kirkham DH, Flowes GC (1974) Am J Sci **274:** 1089-1098.
48. Helgeson HC, Kirkham DH, Flowes GC (1981) Am J Sci **281:** 1249-1516.
49. Johnson JW, Oelkers EH, Helgeson HC (1992) Comput Geosci **18:** 899-947.
50. Kobylin PM (2011) Proceedings of the European Metallurgical Conference **3:** 957-974.
51. Sippola H (1992) *Solubility of ferrous sulphate in sulphuric acid – a thermodynamic model*. Licentiate's Thesis. Helsinki University of Technology 1992.
52. Matsushima Y, Okuwaki A (1988) Bull Chem Soc Jpn **61:** 3344-3346.
53. DeKock, CW (1982) Bureau of Mines, Information Circular 8910.
54. Cox JD, Wagman DD, Medvedev VA (1989) CODATA key values for thermodynamics, Hemisphere Pub. Corp., New York.
55. Glushko VP, et al (1982) Thermodynamic Properties of Individual Substances, Vol 1, Part 2, Nauka, Moscow.
56. Silvester LF, Pitzer KS (1978) J Solution Chem **7:** 327-337.
57. Kobylin PM, Taskinen PA (2012) Calphad **38:** 146-154.
58. Kobylin PM, Taskinen PA (2011) Calphad **35:** 499-511.

59. Sippola H (2012) Thermochim Acta **532:** 65-77.
60. Höffler F, Müller I, Steiger M (2018) J Chem Thermodynamics **116:** 279-288.